EBioMedicine 7 (2016) 248–254

Contents lists available at ScienceDirect

EBioMedicine

journal homepage: www.ebiomedicine.com

Research Paper

First-in-man Safety and Efficacy of the Adipose Graft Transposition Procedure (AGTP) in Patients With a Myocardial Scar

Antoni Bayes-Genis [a,b,c,*], Paloma Gastelurrutia [c], Maria-Luisa Cámara [d], Albert Teis [a,e], Josep Lupón [a,b], Cinta Llibre [a], Elisabet Zamora [a], Xavier Alomar [e], Xavier Ruyra [d], Santiago Roura [c,f], Ana Revilla [g], José Alberto San Román [g], Carolina Gálvez-Montón [c]

[a] Cardiology Service, Germans Trias i Pujol University Hospital, Badalona, Spain
[b] Department of Medicine, Universitat Autònoma de Barcelona, Barcelona, Spain
[c] ICREC Research Program, Health Science Research Institute Germans Trias i Pujol, Badalona, Spain
[d] Cardiac Surgery Service, Germans Trias i Pujol University Hospital, Badalona, Spain
[e] Clínica Creu Blanca, Barcelona, Spain
[f] Center of Regenerative Medicine in Barcelona, Barcelona, Spain
[g] ICICORELAB, Clinic University Hospital, Valladolid, Spain

ARTICLE INFO

Article history:
Received 5 February 2016
Received in revised form 16 March 2016
Accepted 17 March 2016
Available online 10 April 2016

Keywords:
Myocardial infarction
Adipose tissue
Stem cell therapy
Cardiac tissue engineering
Regenerative medicine
Cardiac surgery

ABSTRACT

Background: The present study evaluates the safety and efficacy of the Adipose Graft Transposition Procedure (AGTP) as a biological regenerative innovation for patients with a chronic myocardial scar.
Methods: This prospective, randomized single-center controlled study included 10 patients with established chronic transmural myocardial scars. Candidates for myocardial revascularization were randomly allocated into two treatment groups. In the control arm (n = 5), the revascularizable area was treated with CABG and the non-revascularizable area was left untouched. Patients in the AGTP-treated arm (n = 5) were treated with CABG and the non-revascularizable area was covered by a biological adipose graft. The primary endpoint was the appearance of adverse effects derived from the procedure including hospital admissions and death, and 24-hour Holter monitoring arrhythmias at baseline, 1 week, and 3 and 12 months. Secondary endpoints of efficacy were assessed by cardiac MRI.
Findings: No differences in safety were observed between groups in terms of clinical or arrhythmic events. On follow-up MRI testing, participants in the AGTP-treated arm showed a borderline smaller left ventricular end systolic volume (LVESV; p = 0.09) and necrosis ratio (p = 0.06) at 3 months but not at 12 months. The AGTP-treated patient with the largest necrotic area and most dilated chambers experienced a noted improvement in necrotic mass size (−10.8%), and ventricular volumes (LVEDV: −55.2 mL and LVESV: −37.8 mL at one year follow-up) after inferior AGTP.
Interpretation: Our results indicate that AGTP is safe and may be efficacious in selected patients. Further studies are needed to assess its clinical value. (ClinicalTrials.org NCT01473433, AdiFlap Trial).

1. Introduction

Cardiovascular disease remains the most common cause of mortality worldwide, accounting for more than 17 million deaths annually (Anon., 2011). Myocardial infarction (MI) leads to irreversible myocardial sequelae, often causing debilitating symptoms and shortening life span. Recently, biological regenerative innovations have been introduced as promising therapeutic options (Soler-Botija et al., 2012; Gálvez-Montón et al., 2013a; Prat-Vidal et al., 2014).

Cardiac fat contains a population of mesenchymal-like progenitor cells capable of differentiating into cells that closely resemble cardiomyocytes, both morphologically and molecularly. In murine MI models, these cells improved cardiac function parameters and promoted local neoangiogenesis under hypoxia (Bayes-Genis et al., 2010). The adipose tissue surrounding the heart and pericardium may serve as an autologous biological matrix for salvaging injured myocardium.

The Adipose Graft Transposition Procedure (AGTP) uses patient's existing cardiac fat directly, placing it over the myocardial infarcted zones, rather than explanting a cardiac adipose biopsy to retrieve the cells (Gálvez-Montón et al., 2011; Gálvez-Montón et al., 2013b). In the

* Corresponding author at: ICREC (Heart Failure and Cardiac Regeneration) Research Program, Head of Cardiology Service, Germans Trias i Pujol University Hospital, Crta. Canyet, s/n, 08916 Badalona, Barcelona, Spain.
E-mail address: abayes.germanstrias@gencat.cat (A. Bayes-Genis).

http://dx.doi.org/10.1016/j.ebiom.2016.03.027

acute MI porcine model, functional analyses showed an improvement in LVEF in the AGTP-treated arm five-fold higher than untreated animals (Gálvez-Montón et al., 2011). In the chronic MI porcine model, morphometry revealed a 34% reduction in left ventricular infarct area of AGTP-treated relative to control animals (Gálvez-Montón et al., 2013b). These preclinical studies in a large mammal model suggest that AGTP may be an effective post MI treatment for patients. Accordingly, a prospective randomized trial was set up to assess safety and efficacy of AGTP in patients with a myocardial scar.

2. Patients and Methods

2.1. Patients

The study included 10 candidates for myocardial revascularization with an established chronic transmural myocardial scar, from January 2012 to November 2013. Inclusion criteria included patients ≥18 years of age, with an established transmural MI (minimum three months old) anatomically non amenable for surgical revascularization, and candidates for coronary artery bypass graft (CABG) surgery of other arteries non responsible for the transmural scar. A non-revascularizable area was defined as a chronic transmural necrosis detected by means of late gadolinium enhancement >70% of myocardial thickness on MRI.

Exclusion criteria were: severe valvular disease apt for surgery, candidates to surgical ventricular remodeling, contraindication for MRI, extra-cardiac disease with life expectancy <1 year, severe renal or hepatic insufficiency, previous cardiac surgery, very high surgical risk by EuroSCORE (>8), and pregnant or breastfeeding women.

2.2. Study Design and AGTP Intervention

This study was a prospective, single-center, randomized controlled phase I—II clinical trial (ClinicalTrials.gov number NCT01473433, AdiFLAP Trial). It was designed and implemented in accordance with the Declaration of Helsinki; informed consent was obtained from all participating patients.

Enrolled patients were randomly allocated in 2 arms (Fig. 1):

- Control arm (n = 5): Patients in whom the revascularizable area was treated with CABG and the non-revascularizable area was left untouched.
- AGTP-treated arm (n = 5): Patients in whom the revascularizable area was treated with CABG and the non-revascularizable area was covered by an autologous pericardial adipose graft. Fig. 2 summarizes the steps of the AGTP intervention. First, to obtain the graft, the pericardial adipose tissue was detached with its vascularization intact (depending on scar location, the adipose tissue was detached from the left or the right side of the pericardium as needed); next, after pericardiotomy, the vascular adipose graft was gently positioned to ensure full coverage of the necrotic zone; finally, to secure the flap, the edges were adhered to bordering healthy myocardium with commercially available cyanoacrylic-based surgical glue (Glubran®2, USA) (Gálvez-Montón et al., 2011; Gálvez-Montón et al., 2013b; Bagó et al., 2013; Roura et al., 2015).

The clinical cardiologist handling postsurgical care and the MRI specialist were both blind to the participants' treatment. Study visits consisted of a baseline visit (obtained informed consent and performed clinical assessment, including MRI), surgical intervention, and follow-up visits at one week (clinical assessment), three and 12 months (clinical assessment including MRI) after procedure.

Safety of the procedure was evaluated by the presence of major clinical events including hospital admissions and death, and by the results of a 24-hour Holter monitor test done at each study visit to assess arrhythmias. Efficacy was assessed by left ventricular ejection fraction (LVEF), cardiac output (CO), stroke volume (SV), end-diastolic wall mass (EDWM), left ventricular end-diastolic (LVEDV) and end-systolic volume (LVESV) by means of cardiac-MRI. NTproBNP, troponin I (TnI), NYHA functional class and Framingham derived clinical score were also assessed.

2.3. Cardiac MRI Data Acquisition and Analysis

All imaging were performed in a state-of-the-art 1.5 T clinical imaging system (Avanto; Siemens Medical Imaging, Erlangen, Germany) with the patient in the supine position and a 16-element phased-array coil placed over the chest. Images were acquired during breath-holds with ECG gating. We used a segmented k-space steady-state free-precession sequence [RT 44.70 ms; echo time 1.26 ms; flip angle 78; matrix 272; spatial resolution (1.3–1.5)×(1.3–1.5) × 8 mm depending on the field of view] for cine imaging in parallel short-axis (contiguous slices of 8-mm thickness covering from base to apex) and 3 long-axis views of the left ventricle. Delayed enhancement images were acquired with a segmented gradient-echo inversion-recovery sequence [RT (600–800) ms depending on the cardiac heart rate; echo time 3.24 ms; flip angle 25; matrix 256; spatial resolution 1.3 × 1.3 × 8 mm] at matching cine-image slice locations 10 to 20 min after intravenous gadolinium-DTPA administration (0.20 mmol/kg; Gadovist, Bayer Schering Pharma AG, Berlin, Germany) (Simonetti et al., 2001). We optimized the inversion time to null the normal myocardium and adjusted views per segment and trigger delay according to the patient's heart rate. Native and post contrast cardiac T1 mapping was calculated using a modified Look–Locker inversion recovery sequence (MOLLI) in a short axis view at the infarct level (Moon et al., 2013; White et al., 2013; Messroghli et al., 2004, 2007).

All images were reviewed and analyzed off-line with a specialized post-processing software (QMass-MR, v.7·0; Medis Medical Imaging

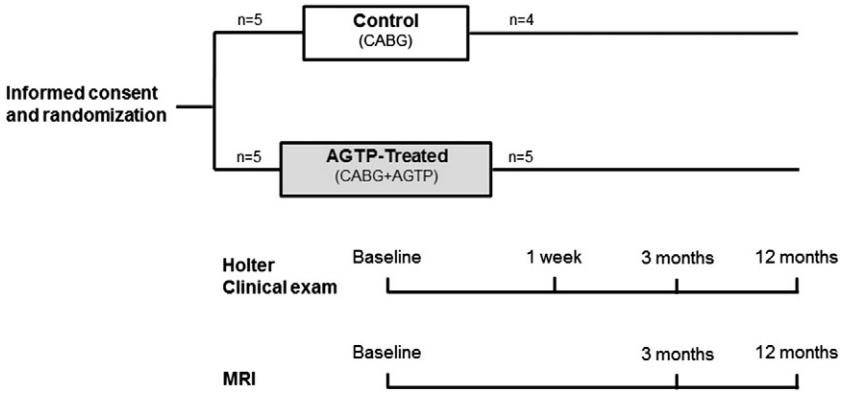

Fig. 1. Study design. n: number of patients, CABG: coronary artery bypass graft, AGTP: Adipose Graft Transposition Procedure, MRI: magnetic resonance imaging.

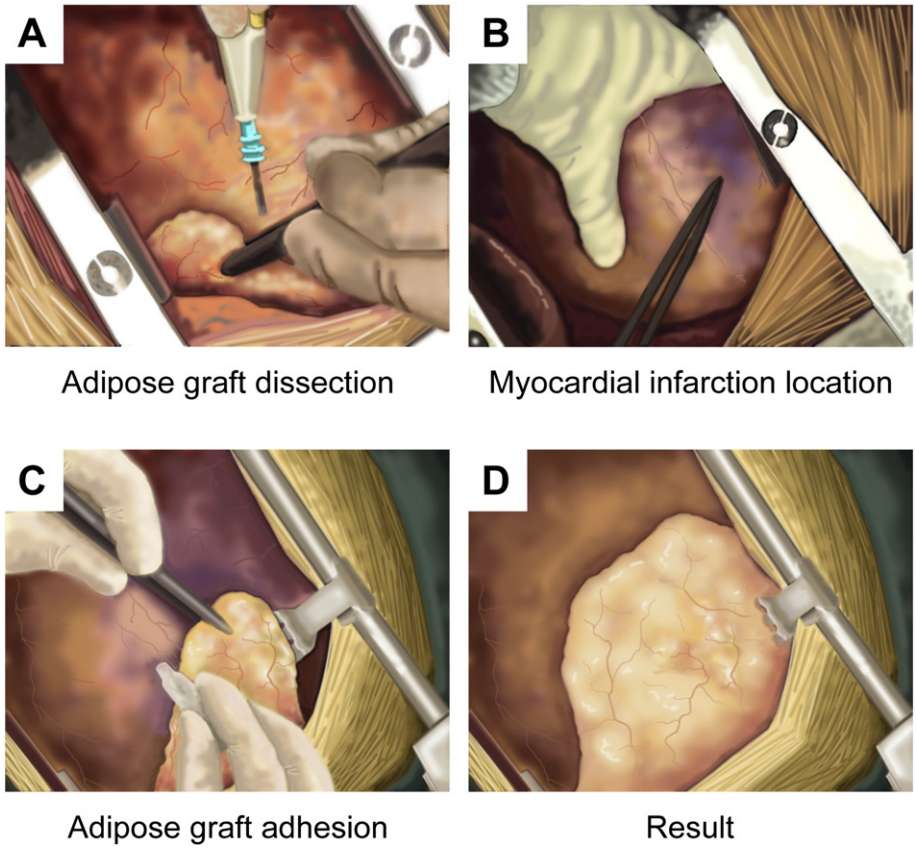

Fig. 2. Schematic illustration of the Adipose Graft Transposition Procedure (AGTP). Pericardial adipose tissue is dissected to create the graft (A). After partial pericardiectomy, MI is located (B) and the pericardial adipose graft is transposed onto the infarct area and glued on healthy edges (C), covering the ischemic myocardium (D). The figure was designed and hand-drawn by CG-M.

Systems, Leiden, the Netherlands) by an independent core lab, which collected and interpreted all imaging data blinded to the clinical data and outcome (J.A.S., A.R.: ICICORELAB, Valladolid, Spain; A.T.). LV endocardial border (papillary muscles were excluded) were manually traced on all short-axis cine images at the end-diastolic and end-systolic frames to determine the LV end-diastolic and LV end-systolic volumes, respectively. LV mass was calculated by subtracting the endocardial volume from the epicardial volume at end diastole and then multiplying by the tissue density (1.05 g/mL) (Kramer et al., 2008).

The endocardial and epicardial contours on delayed enhancement images were also outlined manually. ROIs were then manually traced in the hyperenhanced area at place of maximum signal intensity and in the normal-appearing remote myocardium. As previously described, the areas of hyperenhancing myocardium were then automatically segmented by using a full-width at half-maximum (FWHM) algorithm (Flett et al., 2011; Amado et al., 2004). Two corrections were required for all automated ROIs. First, microvascular obstruction (defined as hypointensity within a hyperintense region in patients with infarctions) was adjusted to be included as late gadolinium enhancement (LGE) if present. Second, any obvious blood pool or pericardial partial voluming and artefacts were further removed from the ROI.

Scar volume for each slice was calculated as: area scar × slice thickness. The scar mass was expressed as total scar volume × 1.05 g. The scar percentage of myocardium was also expressed as a percentage of the total myocardial volume: volume scar / volume myocardium × 100.

T1 mapping derived extracellular volume (ECV) of the necrotic area was estimated using the native and post-contrast myocardial and blood pool T1 maps, accounting for the patient hematocrit at the time of exploration. The T1 map ROI was manually traced covering the entire necrotic area avoiding any blood pool or pericardial partial voluming or artefact. Moreover, areas of microvascular obstruction or fatty infiltration were excluded from the T1 mapping calculation in order to avoid any bias (Kellman et al., 2015).

2.4. Statistical Analysis

Descriptive analyses were performed at the first step. Categorical variables were described by frequencies and percentages. Continuous variables were described by means and standard deviations or medians and interquartile ranges in cases of skewed distribution. Differences between groups were compared using Student's t-test or one-way ANOVA for multiple comparisons, with Tukey's test for *post hoc* analyses. The comparison of continuous variables between groups was performed using analysis of variance for unpaired data once normality was demonstrated (Kolmogorov–Smirnov test); otherwise, a nonparametric test (Mann–Whitney or Kruskal–Wallis test) was used. MRI data were analyzed as repeated measures using ANOVA with Greenhouse–Geisser correction. A 2-sided $p < 0.05$ was considered significant. Statistical analyses were performed using SPSS statistical package 19.0.1 version (SPSS Inc, Chicago, IL, USA).

2.5. Role of the Funding Source

The funding sources had no such involvement.

3. Results

Ten patients were included, randomly allocated to control (n = 5) or AGTP-treated (n = 5). One patient in the control group (Patient #2) was excluded after randomization because of MRI claustrophobia, resulting in a total sample size of n = 9. All patients were men and there were no significant differences between groups in clinical

Table 1
Baseline clinical and MRI variables of the studied population.

	AGTP-treated	Control	p-Value
	N = 5	N = 4	
Age	63.8 ± 13	60.3 ± 6	0.6
Risk factors			
Smoking current/past	2 (40)/3 (60)	3 (75)/1 (25)	0.3
Hypertension	4 (80)	2 (50)	0.3
Diabetes	1 (20)	2 (50)	0.3
Dyslipidemia	4 (80)	1 (25)	0.1
HR	63 ± 7	61 ± 7	0.6
Q wave in ECG	4 (80)	2 (50)	0.3
NYHA I/II/III	0/4 (80)/1 (20)	1 (25)/2 (50)/1 (25)	0.6
NTproBNP	1066 ± 1084	1583 ± 1920	0.7
Peak TnI	3.1 ± 2.8	3.7 ± 2	0.7
Surgical variables			
EuroSCORE	5.4 ± 2.5	3.5 ± 1	0.2
Logistic EuroSCORE, %	5.8 ± 4	2.9 ± 1	0.2
Logistic EuroSCORE II, %	3.1 ± 2.3	1.8 ± 0.9	0.3
Extracorporeal Circ. Time, min	76 ± 13	64 ± 23	0.4
Ischemia time, min	37 ± 25	30 ± 20	0.7
Grafts, nº.	2.2 ± 0.8	2.0 ± 0.8	0.7
MRI variables			
Necrosis mass, gr	34 ± 13	25 ± 4	0.2
Necrosis ratio, %	22 ± 9	18 ± 3	0.4
LVEF, %	41 ± 18	42 ± 15	0.9
LVESV, mL	140 ± 83	128 ± 61	0.8
LVEDV, mL	220 ± 80	212 ± 46	0.8
CO, L/min	5.0 ± 0.8	5.1 ± 1.3	0.9

Data expressed in mean and standard deviation.
AGTP: Adipose Graft Transposition Procedure; HR: heart rate; NYHA: New York Heart Association; NTproBNP: N-terminal pro-B-type natriuretic peptide; ECG: electrocardiogram; TnI: Troponin I; LVEF: left ventricular ejection fraction; LVESV: left ventricular end systolic volume; LVEDV: left ventricular end diastolic volume; CO: cardiac output.

variables, nor in variables related to disease severity or surgical risk (Table 1).

The same surgeon performed all interventions (M.C.). Patency of all grafts was confirmed and no adverse events were detected during surgery. Table 2 summarizes the surgical characteristics of study patients and Video 1 shows an inferior AGTP.

No differences in procedure safety were observed between groups (Table 3). Unrelated to the procedure, one patient died in the AGTP-treated arm after seven months due to colonic adenocarcinoma. There were no differences in hospital admissions during follow-up identified between groups. One hospital admission was registered in each group: in the control arm due to symptomatic hypotension and in the AGTP-treated arm for colonic resection, respectively. 24-hour Holter monitoring during 1-year follow-up showed non-significant differences in arrhythmia prevalence, although the number of supraventricular ectopi in the AGTP-treated arm was reduced (Table 3).

Relative changes in percentage of necrotic tissue from baseline to three months in AGTP-treated and control patients assessed by MRI are shown in Fig. 3. Table 4 shows MRI cardiac function data. Overall, we did not observe significant differences between groups.

Table 3
Safety results.

	AGTP-treated	Control	p-Value
	N = 5	N = 4	
Total adverse events	3	2	0.8
Death	1	0	0.6
Hospital admission	1	1	0.7
New supraventricular arrhythmias[a]	0	0	
New ventricular arrhythmias[a]	1	1	0.9
Changes in number of SVEB[b]	+30 ± 28	+209 ± 731	0.7
Changes in number of VEB[b]	−331 ± 280	−158 ± 218	0.3

AGTP: Adipose Graft Transposition Procedure; SVEB: supraventricular ectopi beats; VEB: ventricular ectopi beats.
[a] Tachycardia defined as three or more beats, taking as reference the pre-intervention 24-h Holter monitoring. Ventricular arrhythmias were asymptomatic non-sustained monomorphic ventricular tachycardia.
[b] Mean number from post-intervention Holter vs. pre-intervention Holter.

However, Greenhouse–Geisser analyses, which include inter- and intra-individual changes over time, did reveal a trend for smaller LVESV ($p = 0.09$) and necrosis ratio ($p = 0.06$) in the AGTP-treated arm at three months. Infarct site-derived T1 mapping extracellular volume (ECV) estimation revealed no significant reduction in the extracellular space from baseline to 3-month follow-up in AGTP-treated versus control patients (−4.5% vs. −1.1%, respectively; $p = 0.53$). No differences in NTproBNP, TnI, NYHA functional class and Framingham-derived clinical score were found between groups.

One patient in the AGTP-treated arm experienced a remarkable improvement after inferior AGTP (Fig. 4). At the beginning of the study, he had the largest necrotic area (LV necrotic mass: 33.2%) and the most dilated ventricular chambers (LVEDV: 315.1 mL; LVESV: 218.5 mL) of all participants; 3 months after AGTP treatment LV necrotic mass was reduced by 4.4%, LVEDV by 31.9 mL, and LVESV by 23.8 mL. After one-year follow-up, these numbers had decreased further to 10.8%, 55.2 mL, and 37.8 mL, for LV necrotic mass, LVEDV, and LVESV respectively. Remarkably, Q waves vanished from leads I, II and III in the follow-up ECGs (Fig. 4).

4. Discussion

The results of this pilot study in a prospective cohort indicate that AGTP is a safe procedure that may be efficacious in selected patients. Given its autologous nature and ease of implementation, the translation of the AGTP technique to clinical practice should not be hampered by technical difficulties, economic restrictions, nor ethical or social considerations.

The mechanism of the positive effects of this biological innovation is uncertain, but one possibility is the establishment of vascular connections between the adipose graft and the underlying myocardium as previously demonstrated in the swine MI model (Bayes-Genis et al., 2013). There are few accepted techniques of vascularizing a damaged heart. In brief, direct methods such as the simple insertion of an internal mammary artery into the myocardium through a hole (Unger et al., 1990)

Table 2
Patient interventional characteristics.

Patient	EuroSCORE	Logistic EuroSCORE[a]	Logistic EuroSCORE II[a]	ECC	ECC time	Ischemia time	Nº grafts	Study arm	AGTP location
1	3	2.40%	1.16%	Yes	92	62	3	AGTP	Inferior
3	8	10.19%	6.69%	Yes	61	32	2	AGTP	Inferior
4	4	3.51%	2.39%	No	–	0	1	Control	–
5	3	2.07%	0.95%	Yes	81	57	3	AGTP	Inferior
6	4	3.76%	1.89%	Yes	89	44	3	Control	–
7	8	10.06%	3.56%	No	–	0	1	AGTP	Inferior
8	4	2.89%	2.44%	Yes	44	32	2	Control	–
9	5	4.38%	3.05%	Yes	70	32	2	AGTP	Anterior
10	2	1.51%	0.58%	Yes	60	42	2	Control	–

ECC: extracorporeal circulation; AGTP: Adipose Graft Transposition Procedure.
[a] Percentage of predicted operative mortality for patients undergoing cardiac surgery by logistic EuroSCORE I and II formulas.

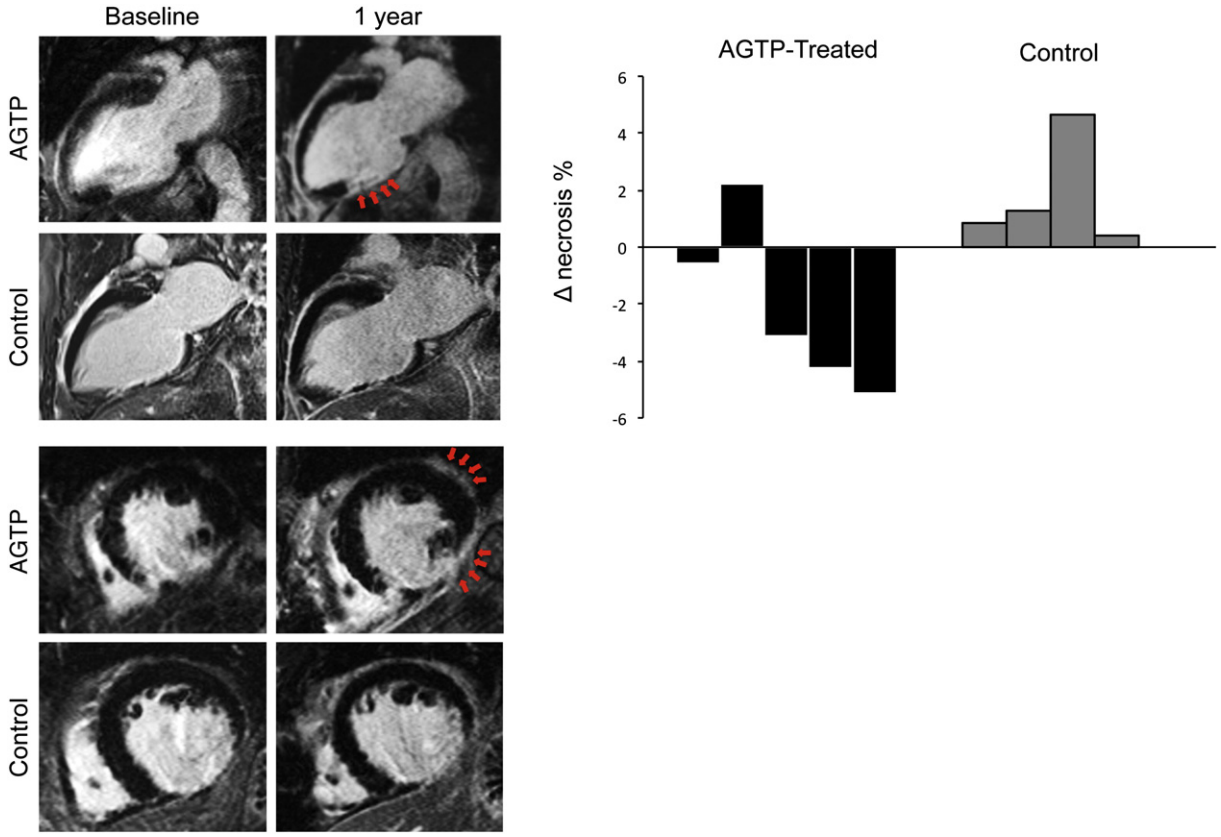

Fig. 3. MRI analysis: Representative T1 short-axis delayed enhancement images rev`eal healthy (black) and infarcted myocardium (white) for AGTP-treated and control patients at baseline and 12 months. Arrowheads point out the attached adipose graft position in the treated patients. Histograms represent changes in percentage of necrotic tissue from baseline to three months in treated and control patients.

or transmyocardial perforation created with lasers mimicking the sinusoids observed in reptilian hearts (Stone et al., 2002) have not demonstrated a clear-cut clinical benefit. In contrast, indirect revascularization of damaged organs with vascular grafts has been successfully achieved (Rocha et al., 2007; Motegi et al., 2007). Previous reports indicate that following AGTP new microvessels developed, bridging the interface between the adipose vascular graft and adjacent myocardium (Gálvez-Montón et al., 2011; Gálvez-Montón et al., 2013b) thus enabling an exchange of nutrients and progenitors between the biological adipose graft and the underlying myocardial scar.

It is unclear whether the adipose-derived progenitor cells exert a role in the beneficial effect of the AGTP. Recent data suggested that cardiac adipose-derived progenitors have an inherent cardiac-like phenotype and may support heart homeostasis, perhaps as a cell reservoir for renewing myocardial tissue. Indeed, in vivo studies in murine models have clearly shown that cardiac adipose-derived progenitors displayed a beneficial effect in the context of MI. Cell transplantation resulted in improved cardiac function parameters and was associated with a significant increase in infarct-related wall thickness (Bayes-Genis et al., 2010). In pre-clinical studies in the porcine model, cell trafficking from the adipose graft to the infarcted myocardium was also observed (Gálvez-Montón et al., 2011). Finally, adipokines liberated by the graft may exert a positive local effect and should be considered as an alternative mechanism. Many studies have described the myocardium and perivascular adipose tissue as well-known sources of hormones, which might exert important autocrine, paracrine, and endocrine effects (Ahima and Flier, 2000). Indeed, evidence suggests that adipose-derived hormones can offer cardio-protective effects, including attenuation of cardiomyocyte apoptosis, reduction of infarct size, and modulation of collagen I/III ratios (Sweeney, 2010).

Identification of AGTP responders is an unresolved challenge, but may ultimately be the key to explaining the case of the AGTP-treated

Table 4
Mean MRI values at baseline, three months and one year follow-up.

	AGTP-treated			Control		
	Baseline	3 months	12 months	Baseline	3 months	12 months
Necrosis mass, gr	33.9	32.9	30.0	25.2	23.8	22.4
Necrosis ratio, %	22.3	20.1	19.3	18.4	20.2	17.8
LVEF, %	41	43	47	42	47	46
LVESV, mL	139.6	131.9	114.9	127.8	99.2	104.6
LVEDV, mL	219.8	218.0	202.4	212.2	187.7	194.6
CO, L/min	5.0	5.5	5.8	5.1	5.9	5.5
SV, mL	80.2	87.3	87.5	84.4	88.5	90.1

Data expressed in mean and standard deviation. No statistically significant differences were observed.
AGTP: Adipose Graft Transposition Procedure; LVEF: left ventricular ejection fraction; LVESV: left ventricular end systolic volume; LVEDV: left ventricular end diastolic volume; CO: cardiac output; SV: stroke volume.

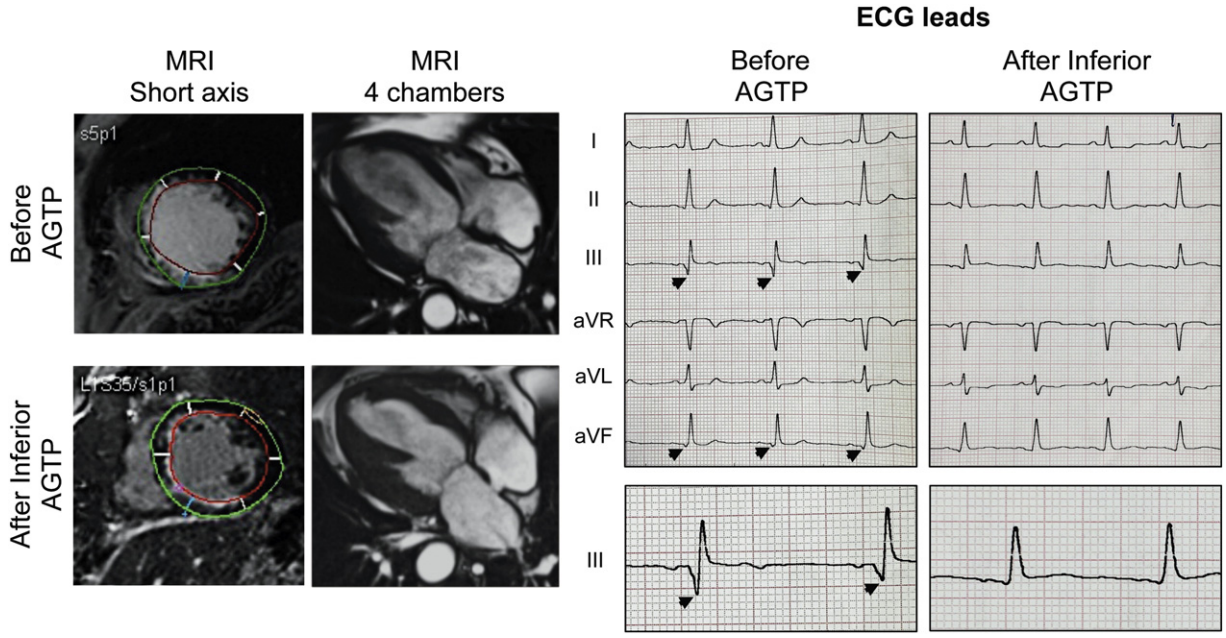

Fig. 4. Selected patient case: short-axis delayed enhanced images show the healthy (black) and infarcted myocardium (white) before and after AGTP; 4-chamber view shows patient's volumes before and after AGTP. Arrows point out the attached adipose graft position in the treated patient. ECG shows a Q wave in leads III and aVF at baseline that is not present at follow-up ECGs.

participant in whom the Q waves vanished. This patient, who demonstrated the most severe indicators at the start of the study, experienced the greatest improvement after AGTP treatment. Further research is required to identify the clinical, biochemical and/or MRI characteristics of AGTP optimal candidates.

AGTP-treated patients showed a trend towards smaller ventricular volumes than the control group. These results should be interpreted with caution; nevertheless it is plausible that AGTP exerted some beneficial effect by the adipose matrix wrapping the infarcted area. However, the associated CABG procedure practiced in these patients should not be discarded.

This study has several limitations. It was a pilot study with a small number of enrolled subjects, limiting our ability to generalize findings to the overall population. We were not able to perform an autopsy of the deceased patient to confirm proper apposition of the graft nor for additional studies at the ultrastructural level. However, the derived T1 mapping ECV estimation may reflect an improvement in scar composition. Furthermore, future MRI software refinements may allow a more precise definition of the adipose graft surrounding the heart.

At present, cell therapy has been the most tested biological approach for cardiac regeneration/recovery in humans. Cell therapy is safe, but with controversial benefits measured in surrogate endpoints such as LVEF. The recent multicenter, prospective, randomized open-label TECAM trial evaluated three different bone marrow-derived stem cell approaches in MI (intracoronary bone-marrow mononuclear cell — BMMC — injection; mobilization with G-CSF; and both BMMC injection plus G-CSF), none of which resulted in improvement of LVEF or volumes compared with standard MI care (San Roman et al., 2015).

This is the first-in-man study on myocardial adipose grafting and we should be restrained in interpreting the results, but findings suggest an improvement in necrosis area in AGTP-treated patients during early follow-up. Future studies are needed to determine whether this innovation translates to superior cardiac function with longer follow-up. This study provides evidence that use of an autologous vascular adipose graft may be a safe alternative in patients with a chronic myocardial scar. A Phase II—III multicenter, prospective, randomized clinical trial is now being set-up to confirm efficacy of the AGTP intervention.

Supplementary data to this article can be found online at http://dx.doi.org/10.1016/j.ebiom.2016.03.027.

Authors' Contributions

Antoni Bayes-Genis: Study concept and design, drafting of the manuscript, critical revision of the manuscript for important intellectual content, recruitment, and final approval of the version to be published.

Paloma Gastelurrutia: Study concept and design, acquisition of data, analysis and interpretation of data, drafting of the manuscript, critical revision of the manuscript for important intellectual content, study supervision, recruitment, and final approval of the version to be published.

Maria-Luisa Cámara: Acquisition of data, recruitment and treatment, final approval of the version to be published.

Albert Teis: Acquisition of data, analysis and interpretation of data, drafting of the manuscript, critical revision of the manuscript for important intellectual content, statistical analysis, final approval of the version to be published.

Josep Lupón: Acquisition of data, analysis and interpretation of data, statistical analysis, final approval of the version to be published.

Cinta Llibre: Analysis and interpretation of data, final approval of the version to be published.

Elisabet Zamora: Acquisition of data, critical revision of the manuscript for important intellectual content, final approval of the version to be published.

Xavier Alomar: Acquisition of data, final approval of the version to be published.

Xavier Ruyra: Study supervision, final approval of the version to be published.

Santiago Roura: Critical revision of the manuscript for important intellectual content, final approval of the version to be published.

Ana Revilla: Acquisition of data, analysis and interpretation of data, final approval of the version to be published.

José Alberto San Román: Acquisition of data, analysis and interpretation of data, final approval of the version to be published.

Carolina Gálvez-Montón: Study concept and design, analysis and interpretation of data, drafting of the manuscript, critical revision of the

manuscript for important intellectual content, statistical analysis, and final approval of the version to be published.

Declaration of Interests

There are no conflicts of interest.

Acknowledgments

This work was supported by grants from the Ministerio de Educación y Ciencia (SAF2014-59892), Ministerio de Economía y Competitividad (Juan de la Cierva, JCI-2012-14025), Fundació La MARATÓ de TV3 (201502-30, 201516-10), Fundació Daniel Bravo Andreu, Casa Tarradellas, Sociedad Española de Cardiología, Societat Catalana de Cardiologia, Generalitat de Catalunya (SGR 2014), and Acadèmia de Ciències Mèdiques i de la Salut de Catalunya i de Balears. This work has also been funded by the Red de Terapia Celular — TerCel (RD12/0019/0029), Red de Investigación Cardiovascular — RIC (RD12/0042/0047) and Fondo de Investigación Sanitaria, Instituto de Salud Carlos III (FIS PI14/01682) projects as part of the Plan Nacional de I + D + I and cofunded by ISCIII-Sudirección General de Evaluación and Fondo Europeo de Desarrollo Regional (FEDER). We specially thank Teresa Sevilla for assistance in MRI image analysis.

References

Ahima, R.S., Flier, J.S., 2000. Adipose tissue as an endocrine organ. Trends Endocrinol. Metab. 11, 327–332.

Amado, L.C., Gerber, B.L., Gupta, S.N., et al., 2004. Accurate and objective infarct sizing by contrast-enhanced magnetic resonance imaging in a canine myocardial infarction model. J. Am. Coll. Cardiol. 44, 2383–2389.

Anon., 2011 April. Burden: mortality, morbidity and risk factors. Global Status Report on Noncommunicable Diseases 2010. World Health Organization, p. 9 (Chapter 1, ISBN: 978 92 4 156422 9).

Bagó, J.R., Soler-Botija, C., Casaní, L., et al., 2013. Bioluminescence imaging of cardiomyogenic and vascular differentiation of cardiac and subcutaneous adipose tissue-derived progenitor cells in fibrin patches in a myocardium infarct model. Int. J. Cardiol. 169, 288–295.

Bayes-Genis, A1., Soler-Botija, C., Farré, J., et al., 2010. Human progenitor cells derived from cardiac adipose tissue ameliorate myocardial infarction in rodents. J. Mol. Cell. Cardiol. 49, 771–780.

Bayes-Genis, A., Gálvez-Montón, C., Prat-Vidal, C., Soler-Botija, C., 2013. Cardiac adipose tissue: a new frontier for cardiac regeneration? Int. J. Cardiol. 167, 22–25.

Flett, A.S., Hasleton, J., Cook, C., et al., 2011. Evaluation of techniques for the quantification of myocardial scar of differing etiology using cardiac magnetic resonance. J. Am. Coll. Cardiol. Img. 4, 150–156.

Gálvez-Montón, C., Prat-Vidal, C., Roura, S., et al., 2011. Transposition of a pericardial-derived vascular adipose flap for myocardial salvage after infarct. Cardiovasc. Res. 91, 659–667.

Gálvez-Montón, C., Prat-Vidal, C., Roura, S., Soler-Botija, C., Bayes-Genis, A., 2013a. Update: Innovation in cardiology (IV). Cardiac tissue engineering and the bioartificial heart. Rev. Esp. Cardiol. 66, 391–399.

Gálvez-Montón, C., Prat-Vidal, C., Roura, S., et al., 2013b. Post-infarction scar coverage using a pericardial-derived vascular adipose flap. Pre-clinical results. Int. J. Cardiol. 166, 469–474 (20).

Kellman, P., Bandettini, W.P., Mancini, C., Hammer-Hansen, S., Hansen, M.S., Arai, A.E., 2015. Characterization of myocardial T1-mapping bias caused by intramyocardial fat in inversion recovery and saturation recovery techniques. J. Cardiovasc. Magn. Reson. 17, 33.

Kramer, C., Barkhausen, J., Flamm, S.D., Kim, R., Nagel, E., 2008. Standardized cardiovascular magnetic resonance imaging (CMR) protocols, society for Cardiovascular Magnetic Resonance: Board of Trustees Task Force on Standardized Protocols. J. Cardiovasc. Magn. Reson. 10, 35.

Messroghli, D.R., Radjenovic, A., Kozerke, S., Higgins, D.M., Sivananthan, M.U., Ridgway, J.P., 2004. Modified Look–Locker inversion recovery (MOLLI) for high-resolution T1 mapping of the heart. Magn. Reson. Med. 52, 141–146.

Messroghli, D.R., Walters, K., Plein, S., et al., 2007. Myocardial T1 mapping: application to patients with acute and chronic myocardial infarction. Magn. Reson. Med. 58, 34–40.

Moon, J.C., Messroghli, D.R., Kellman, P., et al., 2013. Myocardial T1 mapping and extracellular volume quantification: a Society for Cardiovascular Magnetic Resonance (SCMR) and CMR Working Group of the European Society of Cardiology consensus statement. J. Cardiovasc. Magn. Reson. 15, 92.

Motegi, S., Tamura, A., Abe, M., Okada, E., Nagai, Y., Ishikawa, O., 2007. Reverse latissimus dorsi musculocutaneous flap for reconstruction of lumbar radiation ulcer. J. Dermatol. 34, 565–569.

Prat-Vidal, C., Gálvez-Montón, C., Puig-Sanvicens, V., et al., 2014. Online monitoring of myocardial bioprosthesis for cardiac repair. Int. J. Cardiol. 174, 654–661.

Rocha, L.S., Paiva, G.R., de Oliveira, L.C., Filho, J.V., Santos, I.D., Andrews, J.M., 2007. Frontal reconstruction with frontal musculocutaneous V-Y island flap. Plast. Reconstr. Surg. 120, 631–637.

Roura, S., Soler-Botija, C., Bagó, J.R., et al., 2015. Postinfarction functional recovery driven by a three-dimensional engineered fibrin patch composed of human umbilical cord blood-derived mesenchymal stem cells. Stem Cells Transl. Med. 4, 956–966.

San Roman, J.A., Sánchez, P.L., Villa, A., et al., 2015. Comparison of different bone marrow-derived stem cell approaches in reperfused STEMI. A multicenter, prospective, randomized, open-labeled TECAM trial. J. Am. Coll. Cardiol. 65, 2372–2382.

Simonetti, O.P., Kim, R.J., Fieno, D.S., et al., 2001. An improved MR imaging technique for the visualization of myocardial infarction. Radiology 218, 215–223.

Soler-Botija, C., Bagó, J.R., Bayes-Genis, A., 2012. A bird's-eye view of cell therapy and tissue engineering for cardiac regeneration. Ann. N. Y. Acad. Sci. 1254, 57–65.

Stone, G.W., Teirstein, P.S., Rubenstein, R., et al., 2002. A prospective, multicenter, randomized trial of percutaneous transmyocardial laser revascularization in patients with nonrecanalizable chronic total occlusions. J. Am. Coll. Cardiol. 39, 1581–1587.

Sweeney, G., 2010. Cardiovascular effects of leptin. Nat. Rev. Cardiol. 7, 22–29.

Unger, E.F., Sheffield, C.D., Epstein, S.E., 1990. Creation of anastomoses between an extracardiac artery and the coronary circulation. Proof that myocardial angiogenesis occurs and can provide nutritional blood flow to the myocardium. Circulation 82, 1449–1466.

White, S.K., Sado, D.M., Fontana, M., et al., 2013. T1 mapping for myocardial extracellular volume measurement by CMR: bolus only versus primed infusion technique. J. Am. Coll. Cardiol. Img. 6, 955–962.